ChemComm

COMMUNICATION

View Article Online
View Journal | View Issue

Cite this: *Chem. Commun.*, 2016, 52, 7886

Received 1st May 2016,
Accepted 23rd May 2016

DOI: 10.1039/c6cc03627a

www.rsc.org/chemcomm

A Z-scheme photocatalyst constructed with an yttrium–tantalum oxynitride and a binuclear Ru(II) complex for visible-light CO_2 reduction†

Kanemichi Muraoka,[a] Hiromu Kumagai,[a] Miharu Eguchi,[b] Osamu Ishitani*[a] and Kazuhiko Maeda*[a]

An yttrium–tantalum oxynitride having a band gap of 2.1 eV (absorbing visible light at <580 nm) was applicable as a semiconductor component of a Z-scheme CO_2 reduction system operable under visible light, in combination with a binuclear Ru(II) complex that has strong absorption in the visible region (<600 nm). Excitation of this system with visible light under a CO_2 atmosphere induced photocatalytic formation of formic acid with very high selectivity (>99%).

In order to address the depletion of fossil fuels and the concomitant emission of CO_2, the chemical fixation of CO_2 as well as its conversion into useful compounds are currently important topics in the field of chemistry. Various reactions/schemes have been proposed to date for this purpose.[1–12] Among these, photocatalytic CO_2 reduction using a heterogeneous photocatalyst that consists of a semiconductor and a metal complex has great potential because it is a readily scalable process that utilizes only low-density sunlight.[13]

From the viewpoint of solar energy conversion, a semiconductor photocatalyst that harvests a wide range of visible light is highly desirable. Recently, it has been reported that certain metal oxides modified with Ag as a promoter achieved CO_2 reduction using water as the electron source.[7] However, the band gaps of these metal oxides are too large to harvest visible light. While our group has developed heterogeneous photocatalysts for CO_2 reduction that consist of a visible-light-responsive semiconductor and a functional metal complex working as an oxidation and a reduction site, respectively, these novel semiconductors (*e.g.*, TaON, $CaTaO_2N$ and C_3N_4) can harvest visible light only at wavelengths shorter than 500 nm.[9–11] Unfortunately, there are very few semiconductors that have a band gap smaller than 2.5 eV (corresponding to 500 nm wavelength) and that can be applied for photocatalytic CO_2 reduction. Reducing the band gap of a semiconductor will reduce the reactivity of electrons and holes generated in the conduction and valence bands, respectively. At the same time, it will become difficult to satisfy thermodynamic requirements; that is, valence and conduction band potentials that straddle the redox potentials of a desired reaction. Because a CO_2 fixation system using metal-complex/semiconductor hybrid photocatalysts ultimately requires the use of water as the electron source, a semiconductor photocatalyst has to satisfy band edge potentials that straddle both the water oxidation and CO_2 reduction potentials.

Herein we report that an yttrium–tantalum oxynitride (YTON) having a band gap of 2.1 eV coupled with a binuclear Ru(II) complex (**RuRu′**, see Chart 1) works as a photocatalyst for reduction of CO_2 to formic acid under visible-light irradiation. This system works according to the Z-scheme principle; *i.e.*, excitation of both YTON and the redox photosensitizer unit of **RuRu′** with visible light induces reduction of CO_2 to HCOOH with >99% selectivity at room temperature and ambient atmospheric pressure.

The YTON powder was prepared by the conventional thermal ammonolysis of a corresponding Y–Ta oxide precursor that was previously synthesized using the polymerized complex (PC) method. The details of these two procedures are provided

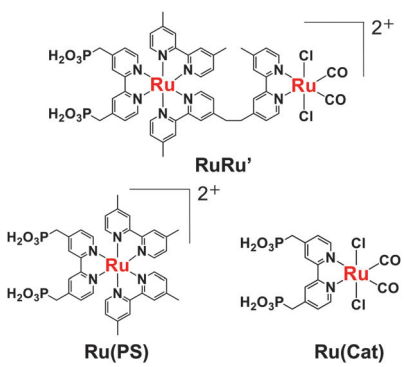

Chart 1 Ruthenium(II) complexes used in this work.

[a] *Department of Chemistry, School of Science, Tokyo Institute of Technology, 2-12-1-NE-2 Ookayama, Meguro-ku, Tokyo 152-8550, Japan. E-mail: ishitani@chem.titech.ac.jp, maedak@chem.titech.ac.jp*
[b] *Electronic Functional Materials Group, Polymer Materials Unit, National Institute for Materials Science, 1-1 Namiki, Tsukuba, Ibaraki 305-0044, Japan*

† Electronic supplementary information (ESI) available. See DOI: 10.1039/c6cc03627a

in the ESI†. The synthesis of single-phase pyrochlore $Y_2Ta_2O_5N_2$ was confirmed by X-ray diffraction (XRD) analysis (Fig. S1, ESI†). Energy-dispersive X-ray (EDX) spectroscopy and thermogravimetric (TG) analysis of the as-prepared YTON determined that the Y/Ta ratio was 0.95, and that the concentration of nitrogen in the material was 1.2 wt%, values that were below the theoretical values (Y/Ta = 1, N: 4.3 wt%), indicating a non-stoichiometric composition. TEM observations showed that the YTON consisted of 20–30 nm primary particles connected to one another to form larger secondary particles with porous structures (Fig. 1A). The specific surface area of the YTON was determined by nitrogen adsorption/desorption to be 16 $m^2\ g^{-1}$, a result that can be attributed to its porous structure. As shown in Fig. 1B, the YTON had an absorption edge at approximately 580 nm, consistent with an earlier report.[14] The band gap of the material was estimated to be about 2.1 eV based on the onset wavelength of its diffuse reflectance spectrum.

Li *et al.* have reported that yttrium–tantalum oxynitride exhibits photocatalytic activity for both water reduction and oxidation under visible light.[14] However, the band-edge potentials of the material have not been reported and remain unclear. Therefore, we conducted photoelectrochemical analyses in order to investigate the band-gap structure.[15] The actual band-edge positions were evaluated by measuring the onset potentials of photocurrents generated from an IrO_2/TiO_2/YTON/FTO electrode in electrolyte solutions with various pH values. In these experiments, the YTON was immobilized on the FTO by a conventional squeegee method and a TiO_2 layer was deposited to improve the inter-particle electron transfer and particle/substrate electron transfer.[15a,16] In addition, colloidal IrO_2 was deposited on the TiO_2/YTON to enhance the water oxidation.[16b]

Current–voltage curves were acquired under chopped visible light irradiation ($\lambda > 500$ nm), scanning from negative to positive potential at 5 mV s^{-1} in an aqueous Na_2SO_4 solution adjusted to pH 4.8, 8.7 or 11.7 by the addition of H_2SO_4 or NaOH. As shown in Fig. S2 (ESI†), an anodic photocurrent attributed to water oxidation was observed under all pH conditions examined, indicating that the YTON functions as an n-type semiconductor. The onset potential, corresponding to the flat-band potential (E_{FB}), was shifted to the negative direction with increasing pH. The energy difference between the conduction band edge potential (E_{CB}) and the E_{FB} is believed to be approximately 0.1–0.3 eV based on the n-type semiconducting character

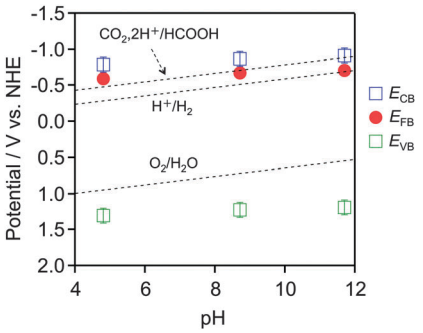

Fig. 2 Dependence of conduction and valence band edge potentials for the as-prepared YTON on the pH of the electrolyte, as determined from photocurrent measurements (see Fig. S2, ESI†).

of the YTON.[17] On the basis of the YTON band gap (2.1 eV), the valence band edge potential (E_{VB}) can be estimated to be 2.1 V more positive than E_{CB}. Fig. 2 presents the conduction and valence band edge potentials of the IrO_2/TiO_2/YTON/FTO electrode as a function of pH. The positions of the YTON conduction band minimum and the valence band maximum evidently vary with pH, and were shifted at a rate of approximately −17 mV per pH as the pH increased. It was thus shown that YTON had band-edge potentials suitable for water oxidation in all pH range examined. Under basic pH conditions, however, it is clear that the driving force for CO_2 reduction becomes insufficient.

Prior to photocatalytic reaction, the YTON was modified with both Ag and **RuRu′** having methylphosphonic-acid anchoring groups, which, respectively, work as a promoter for interfacial electron transfer and as another photocatalytic unit with high capability for CO_2 reduction.[10b,11] TEM observations indicated that metallic Ag nanoparticles approximately 10 nm in size were distributed on the YTON surface (Fig. 3A). The resulting lattice fringe had a period of 0.24 (Fig. 3B), consistent with the *d* spacing of Ag(111) planes. The successful immobilization of **RuRu′** on Ag/YTON was verified by means of Fourier transform infrared (FT-IR) spectroscopy (Fig. S3, ESI†).

Using the as-prepared YTON with Ag and/or **RuRu′**, CO_2 reduction was performed under visible light irradiation ($\lambda > 400$ nm). The reaction setup used in this work was identical to that we have reported previously.[10,11] Table 1 summarizes the results. To avoid complications resulting from water oxidation catalysis,

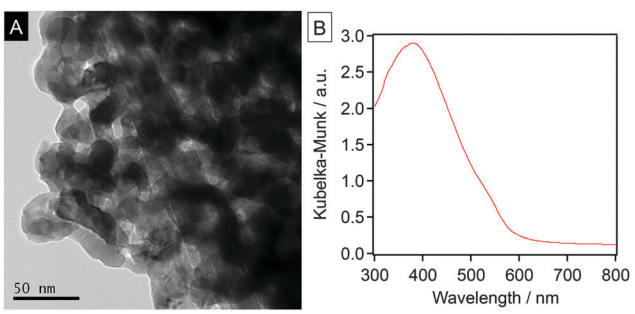

Fig. 1 (A) TEM image, and (B) UV-visible diffuse reflectance spectrum of the as-prepared YTON.

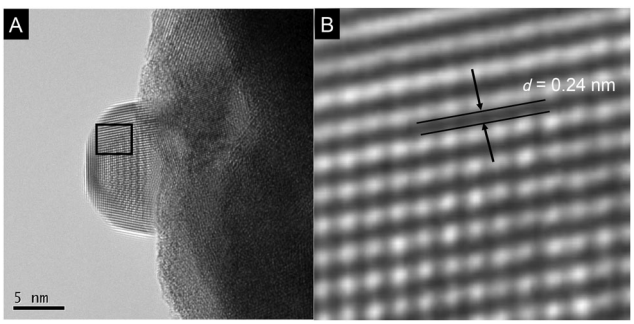

Fig. 3 TEM images of Ag(1.5 wt%)/YTON. Panel B shows a magnified image of the square in panel A.

Table 1 Results of visible-light CO_2 reduction using YTON with various modifications ($\lambda > 400$ nm)[a]

Entry	Photocatalyst	Amount of HCOOH/nmol	TON	Selectivity
1	**RuRu′**/YTON	162	5	>99
2	**RuRu′**/Ag/YTON	630	18	>99
3	YTON	N.D.	—	—
4	Ag/YTON	N.D.	—	—
5	**RuRu′** (6.0 μM)	N.D.	—	—
6[b]	**RuRu′**/Ag/YTON	N.D.	—	—
7[c]	**RuRu′**/Ag/YTON	N.D.	—	—
8[d]	**RuRu′**/Ag/YTON	N.D.	—	—
9	**Ru(PS)**/Ag/YTON	N.D.	—	—
10	**Ru(Cat)**/Ag/YTON	N.D.	—	—

[a] Reaction conditions: photocatalyst, 8.0 mg (Ag 1.5 wt%); solution, a mixture of DMA and TEOA (4 : 1 v/v) 4.0 mL; light source, 400 W high-pressure Hg lamp (SEN) with a $NaNO_2$ solution filter. Reaction time: 24 h. The amount of metal complex loaded in each case was 4.5 μmol g^{-1}. [b] Under an Ar atmosphere. [c] Without TEOA. [d] In the dark.

reactions were conducted in a mixed *N*,*N*-dimethylacetamide (DMA)/triethanolamine (TEOA) solution (4 : 1 v/v), where TEOA worked as a sacrificial electron donor.

Combining YTON with **RuRu′** resulted in clearly observable HCOOH production with very high selectivity (>99%) and catalytic turnover numbers (TON_{HCOOH}) of 5 based on the amount of loaded **RuRu′** (entry 1). The Ag-modification increased the HCOOH formation (TON_{HCOOH} = 18, entry 2). This is attributed to the promotional effect of the Ag, which facilitates interfacial electron transfer from the semiconductor to the excited state of the binuclear Ru(II) complex,[10b,11] as discussed below. The generation of HCOOH over **RuRu′**/Ag/YTON was improved with increases in the amount of Ag loaded, up to 1.5 wt%, beyond which the yield began to decrease (Fig. S4, ESI†). By contrast, neither the YTON nor the Ag/YTON showed activity for the reaction (entries 3 and 4). Note that TEOA cannot reductively quench the photosensitizer unit of **RuRu′**, *i.e.*, it is reasonable that only **RuRu′** without YTON did not induce photocatalytic reduction of CO_2 (entry 5 in Table 1). In the absence of CO_2 or TEOA, no HCOOH production was observed (entries 6 and 7), nor was there any reaction under dark conditions (entry 8). It should be noted that neither CO nor H_2 gas evolution was observed in all cases. No C–C coupling product (*e.g.*, ethane and ethanol) was detected as well. These results show that both YTON and **RuRu′** are essential to realize HCOOH production, and that TEOA works as an electron donor to scavenge holes in the valence band of the YTON.

When using Ag/YTON modified with either a model mononuclear complex of the redox photosensitizer unit (**Ru(PS)**) or the catalytic model complex (**Ru(Cat)**), no HCOOH production could be detected (entries 9 and 10). **Ru(Cat)** has been shown to function as a cocatalyst for CO_2 reduction to generate HCOOH on certain semiconductors (such as C_3N_4 and $CaTaO_2N$),[9,10b] but it was evidently not effective in conjunction with YTON, probably because of the lower conduction-band potential.

Fig. 4 presents an energy diagram for **RuRu′**/YTON based on the results of photoelectrochemical measurements (Fig. 2) and our previous study.[10a] Upon visible light irradiation ($\lambda > 400$ nm), both the YTON and the photosensitizing unit of the **RuRu′**

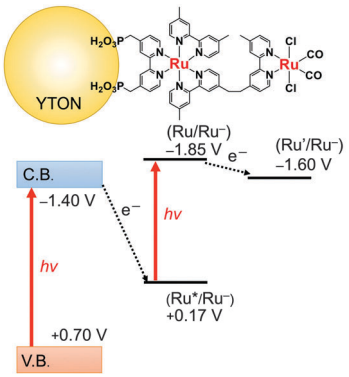

Fig. 4 Energy diagram of **RuRu′**/YTON.

undergo excitation. In this case, it should be noted that electron transfer from the excited state of **RuRu′** (E_{ox}^* = −1.30 V) to the conduction band of the YTON (−1.40 V) is energetically unfavourable. This energy diagram explains the observation that **Ru(Cat)**/YTON did not promote the photocatalysis of the CO_2 reduction (Table 1, entry 10), because the electron transfer from the conduction band of YTON (−1.40 V) to **Ru(Cat)** (−1.60 V) is energetically unfavourable. Conversely, the driving force for electron transfer from the conduction band of YTON to the excited state of **RuRu′** (+0.17 V) is very large (*i.e.*, ΔE = 1.57 V). This reductive electron transfer path appears to be the key to achieving CO_2 reduction. In fact, we were able to observe reductive electron transfer by investigating the lifetime of the excited state of **Ru(PS)** immobilized on the Ag/YTON surface. Fig. 5 presents the emission decay curves of **Ru(PS)** adsorbed on YTON with various loading amounts of Ag during excitation at λ_{ex} = 444 nm. In these experiments, both the YTON and **Ru(PS)** underwent photoexcitation, and increasing the loading amount of Ag accelerated the emission decay of the excited state of **Ru(PS)**. It is noteworthy that oxidative quenching of the excited state of the **Ru(PS)** did not occur, as discussed above. Previously, we have confirmed that electron- and/or energy-transfer from the excited state of **Ru(PS)** to Ag is negligible.[11] Therefore, the evidently enhanced emission quenching is attributed to the acceleration of the reductive quenching of the excited state of **Ru(PS)** by YTON as well as facilitation of the interfacial electron transfer between the YTON and **Ru(PS)** by the added Ag.

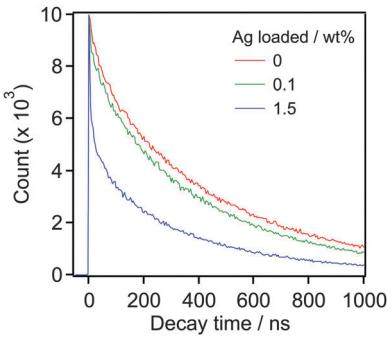

Fig. 5 Emission decay profiles of **Ru(PS)**/Ag/YTON with different Ag loading in MeCN.

In any photocatalytic CO_2 reduction experiments, it is essential to investigate the origin of the carbon source(s) in the reaction product(s), because these may result from surface contaminants such as hydrocarbons and organic acids.[18] Therefore, we performed the reduction of ^{13}C-labeled CO_2 in a similar manner to the previous trials. After 60 h of visible light irradiation, the reacted suspension was filtered and the supernatant was analysed by ^1H NMR spectroscopy. As shown in Fig. S5 (ESI†), a doublet centred at δ = 8.42 ppm with a coupling constant of $J^{13}{}_{CH}$ = 192 Hz was observed, attributed to a proton bound to the ^{13}C atom in $H^{13}COOH$. The observed coupling constant is consistent with that reported in our previous work.[9a] In addition to the doublet, a singlet peak appeared at δ = 8.42 ppm, which was attributed to $H^{12}COOH$. This singlet was also observed when the reaction was conducted in the dark, indicating that $H^{12}COOH$ detected was not generated photocatalytically but rather resulted from contaminants, as indicated by our previous study.[10b] Here, approximately 50% of HCOOH generated came from CO_2. XRD analysis also showed that no change in the XRD pattern of **RuRu**/Ag/YTON before and after reaction (Fig. S1, ESI†). On the basis of these results, it is concluded that the production of HCOOH over **RuRu′**/Ag/YTON hybrid proceeds *via* CO_2 reduction driven by the two-step photoexcitation of both YTON and the light-harvesting Ru complex in **RuRu′**.

In summary, we developed a new semiconductor material for a Z-scheme photocatalyst coupled with a binuclear Ru(II) complex, *i.e.*, an yttrium–tantalum oxynitride having a band gap of 2.1 eV. This hybrid photocatalyst can reduce CO_2 to HCOOH with a very high selectivity (>99%).

This work was supported by the PRESTO/JST program "Chemical Conversion of Light Energy" and a Grant-in-Aid for Young Scientists (A) (Project 16H06130). The support from a Grant-in-Aid for Scientific Research on Innovative Area "Artificial Photosynthesis (AnApple)" (JSPS), the Photon and Quantum Basic Research Coordinated Development Program (MEXT, Japan), and a CREST program (JST) is also gratefully acknowledged. Finally, K. M. wishes to thank the Noguchi Institute and the Murata Science Foundation for financial support.

Notes and references

1 (*a*) T. Ohkawara, K. Suzuki, K. Nakano, S. Mori and K. Nozaki, *J. Am. Chem. Soc.*, 2014, **136**, 10728–10735; (*b*) T. Suga, H. Mizuno, J. Takaya and N. Iwasawa, *Chem. Commun.*, 2014, **50**, 14360–14363.
2 G. Qi, Y. Wang, L. Estevez, X. Duan, N. Anako, A. A. Park, W. Li, C. W. Jones and E. P. Giannelis, *Energy Environ. Sci.*, 2011, **4**, 444–452.
3 (*a*) H. Hori, F. Johnson, K. Koike, O. Ishitani and T. Ibusuki, *J. Photochem. Photobiol., A*, 1996, **96**, 171–174; (*b*) J. Smieja and C. P. Kubiak, *Inorg. Chem.*, 2010, **49**, 9283–9289; (*c*) L. W. Christina, C. Jim and W. K. Matthew, *Nature*, 2014, **508**, 504–507.
4 (*a*) T. Arai, S. Sato, T. Kajino and T. Morikawa, *Energy Environ. Sci.*, 2013, **6**, 1274–1282; (*b*) G. Sahara, R. Abe, M. Higashi, T. Morikawa, K. Maeda, K. Ueda and O. Ishitani, *Chem. Commun.*, 2015, **51**, 10722–10725; (*c*) U. Kang, S. K. Choi, D. J. Ham, S. M. Ji, W. Choi, D. S. Han, A. Abdel-Wahab and H. Park, *Energy Environ. Sci.*, 2015, **8**, 2638–2643.
5 C. Liu, J. J. Gallagher, K. K. Sakimoto, E. M. Nichols, C. J. Chang, M. C. Y. Chang and P. Yang, *Nano Lett.*, 2015, **15**, 3634–3639.
6 (*a*) J. Hawecker, J. M. Lehn and R. Ziessel, *J. Chem. Soc., Chem. Commun.*, 1983, **9**, 536–538; (*b*) H. Takeda, K. Koike, H. Inoue and O. Ishitani, *J. Am. Chem. Soc.*, 2008, **130**, 2023–2031; (*c*) S. Matsuoka, K. Yamamoto, T. Ogata, M. Kusaba, N. Nakashima, E. Fujita and S. Yanagida, *J. Am. Chem. Soc.*, 1993, **115**, 601–609; (*d*) H. Takeda, H. Koizumi, K. Okamoto and O. Ishitani, *Chem. Commun.*, 2014, **50**, 1491–1493; (*e*) H. Takeda, K. Ohashi, A. Sekine and O. Ishitani, *J. Am. Chem. Soc.*, 2016, **138**, 4354–4357.
7 (*a*) K. Iizuka, T. Wato, Y. Miseki, K. Saito and A. Kudo, *J. Am. Chem. Soc.*, 2011, **133**, 20863–20868; (*b*) K. Teramura, X. Wang, S. Hosokawa, Y. Sakata and T. Tanaka, *Chem. – Eur. J.*, 2014, **20**, 9906–9909.
8 S. Sato, T. Morikawa, S. Saeki, T. Kajino and T. Motohiro, *Angew. Chem., Int. Ed.*, 2010, **49**, 5101–5105.
9 (*a*) K. Maeda, K. Sekizawa and O. Ishitani, *Chem. Commun.*, 2013, **49**, 10127–10129; (*b*) K. Maeda, R. Kuriki, M. Zhang, X. Wang and O. Ishitani, *J. Mater. Chem. A*, 2014, **2**, 15146–15151; (*c*) R. Kuriki, K. Sekizawa, O. Ishitani and K. Maeda, *Angew. Chem., Int. Ed.*, 2015, **54**, 2406–2409; (*d*) K. Maeda, R. Kuriki and O. Ishitani, *Chem. Lett.*, 2016, **45**, 182–184; (*e*) R. Kuriki, O. Ishitani and K. Maeda, *ACS Appl. Mater. Interfaces*, 2016, **8**, 6011–6018.
10 (*a*) K. Sekizawa, K. Maeda, K. Domen, K. Koike and O. Ishitani, *J. Am. Chem. Soc.*, 2013, **135**, 4596–4599; (*b*) F. Yoshitomi, K. Sekizawa, K. Maeda and O. Ishitani, *ACS Appl. Mater. Interfaces*, 2015, **7**, 13092–13097; (*c*) A. Nakada, T. Nakashima, K. Sekizawa, K. Maeda and O. Ishitani, *Chem. Sci.*, 2016, DOI: 10.1039/C6SC00586A.
11 R. Kuriki, H. Matsunaga, T. Nakashima, K. Wada, A. Yamakata, O. Ishitani and K. Maeda, *J. Am. Chem. Soc.*, 2016, **138**, 5159–5170.
12 (*a*) S. Wang, W. Yao, J. Lin, Z. Ding and X. Wang, *Angew. Chem., Int. Ed.*, 2014, **53**, 1034–1038; (*b*) S. Wang and X. Wang, *Angew. Chem., Int. Ed.*, 2016, **55**, 2308–2320; (*c*) J. Qin, S. Wang, H. Ren, Y. Hou and X. Wang, *Appl. Catal., B*, 2015, **179**, 1–8.
13 (*a*) K. Maeda and K. Domen, *J. Phys. Chem. Lett.*, 2010, **1**, 2655–2661; (*b*) Y. Yamazaki, H. Takeda and O. Ishitani, *J. Photochem. Photobiol., C*, 2015, **25**, 106–137.
14 M. Liu, W. You, Z. Lei, G. Zhou, J. Yang, G. Wu, G. Ma, G. Luan, T. Takata, M. Hara, K. Domen and C. Li, *Chem. Commun.*, 2004, 2192–2193.
15 (*a*) K. Maeda and K. Domen, *J. Catal.*, 2014, **310**, 67–74; (*b*) A. Ishikawa, T. Takata, J. N. Kondo, M. Hara and K. Domen, *J. Phys. Chem. B*, 2004, **108**, 11049–11053; (*c*) K. Ogisu, A. Ishikawa, Y. Shimodaira, T. Takata, H. Kobayashi and K. Domen, *J. Phys. Chem. C*, 2008, **112**, 11978–11984.
16 (*a*) N. Nishimura, B. Raphael, K. Maeda, L. Le Gendre, R. Abe, J. Kubota and K. Domen, *Thin Solid Films*, 2010, **518**, 5855–5859; (*b*) K. Maeda and K. Domen, *Angew. Chem., Int. Ed.*, 2012, **51**, 9865–9869.
17 (*a*) D. E. Scaife, *Sol. Energy*, 1980, **25**, 41–54; (*b*) Y. Matsumoto, *J. Solid State Chem.*, 1996, **126**, 227–234.
18 T. Yui, A. Kan, C. Saitoh, K. Koike, T. Ibusuki and O. Ishitani, *ACS Appl. Mater. Interfaces*, 2011, **3**, 2594–2600.